JOURNAL OF MATERIALS SCIENCE 26 (1991) 4008–4021

Tensile properties of high-purity nickel stressed in alkali metal environments

M. G. NICHOLAS, P. J. FERNBACK
Materials Development Division, Harwell Laboratory, Didcot, Oxfordshire OX11 ORA, UK

Tensile failure of high-purity (99.99%) nickel varied systematically with the chemistry of alkali metal environments. Failure was by microvoid coalescence when stressed to destruction in argon, caesium, rubidium and potassium at 250 °C. The ultimate tensile strengths were about 250 MPa and the elongations at failure were approximately 45%. The fracture surfaces of samples tested in sodium displayed evidence of intergranular and transgranular cleavage, but the strength and ductility values were similar to those of samples tested in argon. However, failure in lithium was predominantly by intergranular cleavage, and the average ultimate tensile strengths and elongations to failure were only 107 MPa and 6%. Intergranular cleavage and severe embrittlement was caused also by sodium containing more than 0.2% lithium, but pre-exposure and slow straining had little influence. It is concluded that embrittlement by lithium is a physical process that can be related to parameters such as interfacial energies.

1. Introduction

Liquid alkali metal environments have very varied effects on the mechanical properties of nickel and nickel alloys, and this paper is concerned with the incidence of liquid metal embrittlement (LME). This process, the virtually instantaneous embrittlement that can occur when normally ductile materials are stressed and deformed in a molten metal, can be distinguished from other environmental degradation processes not only by its rapidity (cracks can propagate at several m sec^{-1}) but also by the fact that it can occur even, and indeed preferentially, with chemically unreactive systems. LME of unreactive systems was the first type to be investigated and remains its simplest and classical form; in essence the effect is regarded as brittle fracture induced by a lowering of the surface energy of the solid when contacted by a wetting liquid. This and other forms and effects of liquid metal embrittlement have been described in literature stretching back over a century [1] and have been reviewed several times in recent years [2–8].

Essentially, the liquid metal-induced brittle fracture model argues that the influence of liquid metal environments on the energy of new crack surfaces determines whether or not embrittlement occurs. It is recognized that surface creation is not the only or even the largest energy-demanding process to occur during cracking, but it is argued that it is the controlling factor. As shown in Fig. 1, the crack surface energy can be equated to that of a free metal surface, γ_{SV}, in a vacuum or similar inert environment and to the solid–liquid interfacial energy, γ_{SL}, in a molten metal environment. If the liquid wets the solid, it follows from the Young equation that γ_{SL} is less than γ_{SV}, and the liquid will penetrate the propagating crack. If γ_{SL} is sufficiently low, it is argued that the solid will fail by brittle cleavage rather than by ductile tearing. Further, failure along grain boundaries will be favoured because both the absolute and the proportional energy decrease will be even greater.

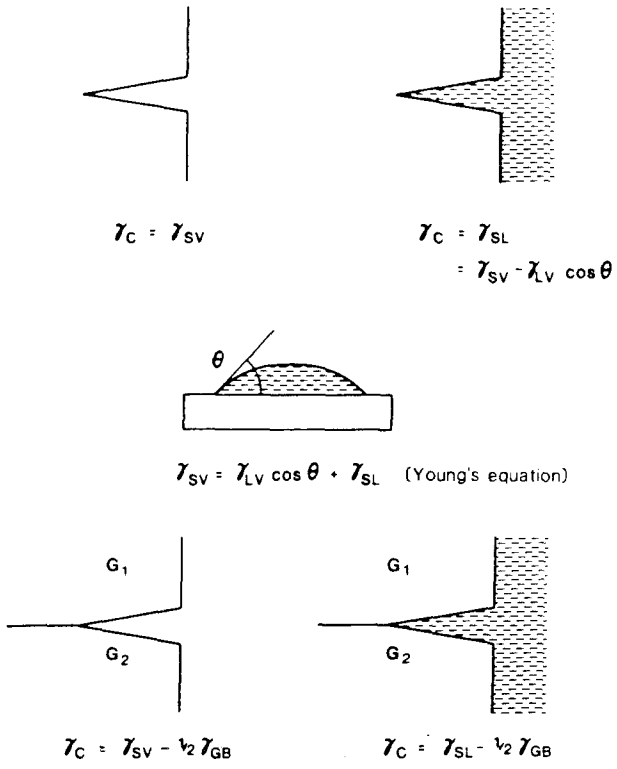

Figure 1 Energy values in liquid metal embrittlement.

The possibility of LME induced by alkali metals is of particular interest to the nuclear industry because of the coolant roles of lithium and sodium in fusion and fast reactors. Additionally, rubidium and caesium can be generated as decay and fission products. It is of

0022–2461/91 $03.00 + .12

concern, therefore, that lithium and, to a lesser extent, sodium have been identified as embrittling species. Even with a very ductile metal such as nickel, the effect of lithium can be severe. An early paper by Parikh [9] reported that 99.9% pure nickel failed in lithium at stresses less than that needed to cause yielding, plastic deformation, and more recently Lynch [10] found that 99.5% pure nickel was severely embrittled and produced fracture surfaces that were 98% intergranular. Lithium has been reported also to embrittle iron and ferritic steels [11–13], copper [14] and nickel–copper alloys [9], but not austenitic stainless steels [15–19]. However, the mechanical degradation of copper and iron is not classical LME, being initiated by the formation of a Cu_4Li intermetallic compound and reaction with carbon in iron grain boundaries to form a voluminous Li_2C_2.

Sodium environments are far more benign. Lynch [10] induced embrittlement of notched tensile test pieces of 99.5% pure nickel, but there was considerable macroscopic plasticity associated with the failures, and the fracture faces were 50% dimpled. Several workers have described studies of the mechanical properties of austenitic [16, 19–21] or ferritic [2, 16, 22] steels in sodium but no detrimental effects have been reported except for some surface decarburization. For the other alkali metals (potassium, rubidium and caesium) no detrimental effects have been reported except for a possible synergistic interaction of caesium and tellurium to embrittle AISI 316 [23], while one study found rubidium and caesium to enhance the ductility of some austenitic stainless steels and nickel alloys [24] due to their efficiency as coolants [25].

Experience suggests therefore that there is a systematic variation in mechanical effects with alkali metal characteristics, and in an early review of the incidence of LME by Rostoker *et al.* [2], it was argued that the incidence of LME could be related to basic system characteristics. In particular, they related immunity to LME to the ability of the liquid–solid system to form intermetallic compounds or to exhibit significant mutual solubility. Even more simply, Westwood *et al.* [26] have related immunity to LME to marked differences in electron negativity.

The lithium–nickel phase diagram displays neither inter-metallic compounds nor significant mutual solubility [27], so a tendency to embrittle might be expected. The Pauling electronegativity value [28] for nickel is 1.8, and those for the alkali metals range progressively from 1.0 for lithium to 0.7 for caesium. These differences are very large and would not normally be associated with embrittlement, but it is noteworthy that the difference is least for lithium and therefore it could be regarded as potentially the most likely embrittling alkali metal.

It is apparent from the experimental data cited earlier that there is a tendency for alkali metal environments to become more benign with increasing atomic number. However, this conclusion is based primarily on observations with alloys and impure nickel. Because iron is embrittled by lithium only when its carbon content exceeds 0.007% and Li_2C_2 is formed, a similar effect may account for the reported severity of lithium-induced LME of nickel. To avoid such effects and cast light on basic material interactions, it was decided to perform a series of tests with high-purity nickel stressed to destruction in argon and in each of the alkali metals, but most particularly lithium and sodium.

2. Materials and techniques

The nickel used in this work was the High Purity grade supplied by Goodfellows Ltd, Cambridge, UK. It had a nominal impurity level of no more than 100 p.p.m. including 15 p.p.m. iron, 3 p.p.m. copper, 2 p.p.m. silica, 1 p.p.m. aluminium, calcium and silver, and less than 1 p.p.m. chromium, magnesium, manganese and tin. Subsequent chemical analysis at Harwell provided confirmation with a measured iron level of 2 p.p.m., and less than the detection levels of aluminium, calcium, chromium, copper, magnesium, manganese and silver. The carbon content was 20 p.p.m.

Most of the alkali metals were obtained from Koch-Light Ltd, Haverhill, UK, but the 99.97% pure potassium came from Goodfellows Ltd. The purities of the other metals were 99.98% for caesium, 99.9% for rubidium, 99.95% for sodium and lithium. Analysis at Harwell confirmed these purity levels and and identified calcium as being the most significant impurity in lithium (300 p.p.m.) and sodium (230 p.p.m.). When needed, sodium–lithium alloy melts were prepared by melting appropriate proportions of the pure metals in a nickel crucible located in a glove box facility. Subsequent analysis of some alloy samples confirmed that there was no significant loss of either component, although the lithium distribution in dilute alloys was rather variable.

The nickel was machined into tensile test pieces with gauge lengths of 15 mm and diameters of 3 mm, as sketched in Fig. 2. Care was taken to achieve a good surface finish along the gauge length and surface profilometry surveys, using an AMS Surfcom 30B machine, indicated that average surface roughness, R_a, values of less than 0.2 μm were achieved. The samples were annealed for 24 h at 1000 °C in argon to produce uniform equiaxed grains ranging in size from 294 to 205 μm with a mean of 233 μm. Before being used in the tensile tests, the nickel samples were cleaned by ultrasonic agitation in acetone for 5 min and then dried using a hot air blast.

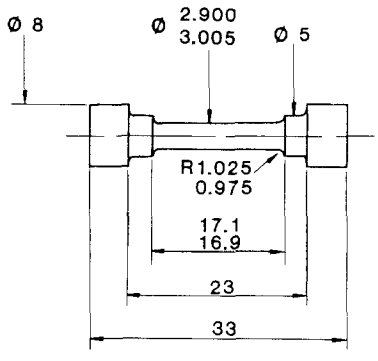

Figure 2 Geometry of tensile test piece (ϕ = diameter; R = radius).

The nickel samples were then loaded into capsules, such as that shown in Figs 3 and 4, in which the tensile tests were performed. The capsule body and pull rod were made of AISI 321 steel but the sample grips and bucket arrangement shown in Fig. 4 were of nickel. The capsules were loaded with the tensile test samples after having been posted into a high integrity, stainless steel bodied, Lintott glove box filled with argon purified to less than 1 v.p.m. water or oxygen. Molten alkali metal or sodium–lithium alloy was prepared in the glove box and injected into the capsule bucket in sufficient quantity to immerse the nickel sample and the pull rod was attached. Then the capsule was sealed and posted out of the glove box. If the subsequent tensile testing was to be done in argon, the capsule was still loaded and sealed in the glove box.

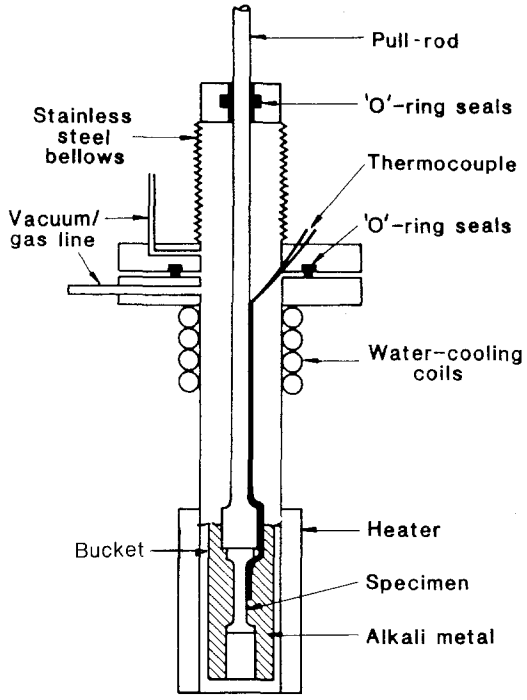

Figure 3 Schematic diagram of mechanical test capsule.

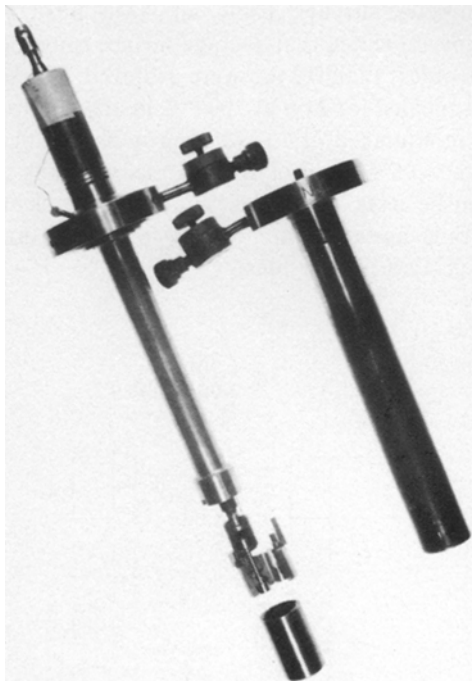

Figure 4 Photograph of mechanical test capsule.

The loaded capsules were fitted to an Instron 1195 tensile test machine, a muffle furnace was slid over the lower body of the capsule and a water-cooled block was bolted to the top flange of the capsule to preserve the "O" ring seals. The capsules were evacuated and refilled with 1 bar of fresh high-purity argon from a train that permitted relief of argon overpressures generated when the capsules were heated. The most common heating cycle involved an initial ramp to 450 °C, following the practice found to be desirable to ensure good wetting of steels by sodium [16]. This was followed by cooling to the tensile test temperature of 250 °C. A sheathed chromel–alumel thermocouple was used to monitor the temperature throughout the cycle and to check whether the temperature had stabilized at 250 ± 1.5 °C during a 10 min dwell prior to stressing. Instron cross-head speeds of 0.05 to 1.00 mm min^{-1} were used with the sample extension being accommodated by the bellows attached to the top flanges of the capsules. The bellows were very soft, adding only an extra 1 N to the failure loads that ranged from 1800 to 700 N. The load extension characteristics of each test were recorded and used to determine the ultimate tensile strength (UTS) values for the samples and make a preliminary estimate of their elongation to failure (E_f). The final values of E_f reported later were determined from direct observation of the samples after they had been removed from the capsules and cleaned.

The capsules were posted back into the glove box for unloading. When necessary, the bottom halves of the samples were eased out of the capsule buckets by remelting the alkali metals. Adherent alkali metal was removed from the sample surfaces by dissolution in ethanol. This method was used also to clean the bucket and other capsule fittings once the bulk of the alkali metal had been remelted and decanted. The dimensions of the unloaded samples were measured, and their fracture surfaces were examined using a Hitachi scanning electron microscope fitted with an EDAX attachment and operated at 25 kV.

This procedure was adopted during the majority of the experiments, each of which was at least duplicated. Variations employed in a minority of experiments will be described when their results are reported.

3. Results

Every sample was well wetted when observed during unloading. Thus the essential requisite for LME, metal–metal contact, was satisfied in every experiment.

Eighteen different conditions were employed in the tensile testing of the nickel samples. The conditions employed and their effects on mechanical properties are summarized in Table I. For clarity, the results of the tests will be reported under four headings.

TABLE I

Environment	Pre-exposure time at 450 °C (min)	Exposure time at 250 °C (min)	Extension rate (mm min^{-1})	Average UTS (MPa)	Average E_f (%)
Ar	15	10	1	246.9 ± 3.7	42.4 ± 1.4
Li	15	10	1	107.5 ± 6.9	6.05 ± 0.45
Na	15	10	1	245.5 ± 9.2	40.0 ± 0.35
K	15	10	1	248.2 ± 7.4	43.7 ± 3.2
Rb	15	10	1	256.7 ± 3.5	46.7 ± 3.6
Cs	15	10	1	244.1 ± 6.3	45.7 ± 2.8
Na*	15	10	1	245.5 ± 9.2	40.0 ± 0.35
Na–0.2 Li	15	10	1	227.9 ± 14.0	32.8 ± 8.4
Na–0.3 Li	15	10	1	212.2 ± 2.8	14.5 ± 0.5
Na–0.6 Li	15	10	1	158.4 ± 1.4	13.3 ± 1.2
Na–2.01 Li	15	10	1	132.3 ± 9.1	11.1 ± 1.6
Na–5.6 Li	15	10	1	124.5	8.7
Li*	15	10	1	107.5 ± 6.9	6.05 ± 0.45
Na–0.2 Li*	15	10	1	227.9 ± 14.0	32.8 ± 8.4
Na–0.2 Li	15	10	0.5	249.0 ± 5.7	43.8 ± 1.5
Na–0.2 Li	15	10	0.2	234.1 ± 0.7	39.2 ± 0.6
Na–0.2 Li	15	10	0.05	207.0 ± 12.6	23.3 ± 5.9
Ar*	15	10	1	246.9 ± 3.7	42.4 ± 1.4
Ar	120	10	1	249.3 ± 4.2	42.1 ± 1.7
Ar	15	960	1	238.7 ± 7.1	41.0 ± 1.3
Na–0.2 Li*	15	10	1	227.9 ± 14.0	32.8 ± 8.4
Na–0.2 Li	120	10	1	241.9 ± 5.6	40.2 ± 3.5
Na–0.2 Li	15	960	1	231.8 ± 1.4	41.7 ± 0.9

* Repeated data.

3.1. Effects of alkali metal environments

Samples were stressed to destruction at 250 °C in argon or alkali metals using an Instron extension rate of 1 mm min^{-1}. A batch of seven samples tested in argon had UTS values of 246.9 ± 3.7 MPa and elongations to fracture, E_f, of 42.4 ± 1.4%. These strength values were closely matched by those observed during tests in molten sodium, potassium, rubidium and caesium, Fig. 5, but the UTS of samples tested in lithium only averaged 107.5 ± 6.9 MPa. The E_f values for samples tested in caesium, potassium and rubidium environments (Fig. 5) were slightly higher than that for argon but the average E_f of 40% in sodium was slightly lower, and that of 6.05% in lithium was much less. However, the load–extension characteristics of the samples prior to failure were similar for all the

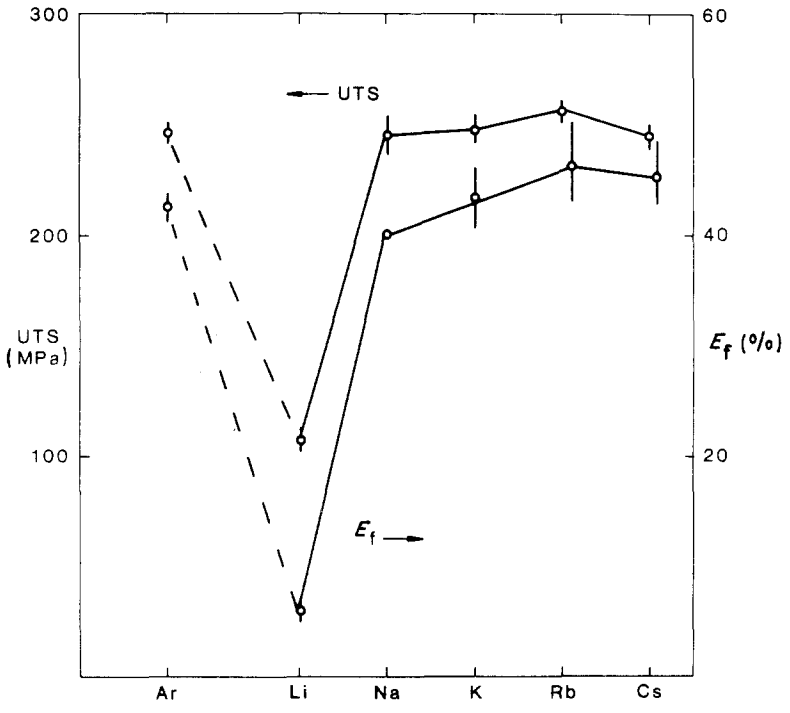

Figure 5 The effect of environment on the ductility of nickel at 250 °C.

environments as illustrated by the examples shown in Fig. 6.

Subsequent examination of the sample fracture surfaces showed that samples tested in argon, potassium, rubidium and caesium had failed in a ductile manner by microvoid coalescence to produce dimpled fracture surfaces such as those shown in Fig. 7. The samples broken in sodium showed evidence of several types of failure. On average, about 20% of the fracture area had failed by intergranular cleavage and about 40% by transgranular cleavage. Samples broken in lithium failed intergranularly except for a small proportion, about 5%, of transgranular cleavage. The surfaces of samples broken in lithium or sodium had populations of adherent cubic crystals, Fig. 8, which EDAX surveys showed to be calcium rich and are believed to be calcium carbonate.

More detailed examination of the samples that failed in a ductile manner in argon, rubidium or caesium, Fig. 9, revealed that the walls of deep dimples were covered with slip markings. The population of dimples increased progressively as larger magnifications were used, but there was only very infrequent evidence that they had been nucleated at inclusions, Fig. 9e. Similarly, more detailed examination of samples broken in sodium revealed the very heavy deformation associated with transcrystalline failure, Fig. 8a. Areas of intergranular failure look unmarked in that micrograph but others revealed evidence of rippling. The micrographs identified as Fig. 8b and c show that rippling occurred also with samples that failed intergranularly in lithium but that the occasional areas of transgranular cleavage were much more heavily deformed.

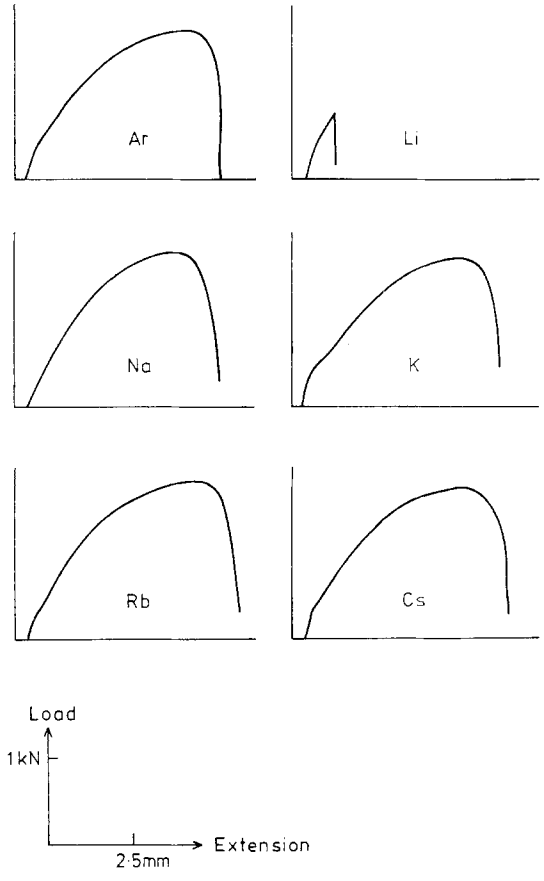

Figure 6 Load–extension curves for nickel samples stressed to destruction at 250 °C in argon and alkali metal environments.

3.2. Effects of sodium–lithium environments

Because lithium is very embrittling but sodium, the other alkali metal of primary nuclear concern, is relatively benign, it was decided to investigate the behaviour of sodium–lithium alloys. The alloys exhibit extensive liquid immiscibility [27], the maximum solubilities at 250 °C being about 8% lithium in sodium and 25% sodium in lithium, and these experiments used sodium as the solvent metal.

Increasing the lithium content of sodium from 0.3% to 5.6% progressively decreased the ductility of nickel from an E_f of 14% to 9%, Table I. As shown by Fig. 10, the E_f values decreased linearly with the logarithm of the lithium concentration and the plot can be extrapolated to accommodate the ductility observed in a pure lithium environment. However, when a batch of ten samples was tested in melts of sodium–0.2% lithium (the most dilute alloy it was practical to prepare in a reproducible manner) a marked but variable ductility increase was observed suggesting that the lithium concentration was close to an embrittlement threshold.

The UTS values for the nickel samples also decreased as the lithium contents of the melts was raised as shown in Fig. 11. Although substantial, the effect was less dramatic than that on the ductility. There was no obvious threshold for weakening but the most marked effect occurred when the lithium content of the melts was increased from 0.3% to 0.6%.

Fracture characteristics also were affected by the lithium contents of the melts, with changes that reflected the variation of E_f values. Fig. 12 shows that the fracture of samples tested in sodium–0.2% lithium were variable; a sample which had an E_f of 25.8% failed predominantly by intergranular cleavage while another with an E_f of 40% produced a fracture surface displaying both intergranular and transgranular cleavage as well as some dimples. However, as shown in Fig. 13 samples tested in sodium containing 0.3% or more of lithium failed consistently by predominantly intergranular cleavage.

3.3. Strain-rate effects

Further experiments with sodium–0.2% lithium environments were conducted in which the Instron cross-head speed was decreased from 1 to 0.05 mm min^{-1}, corresponding to a strain-rate decrease from 1.1×10^{-3} to 5.5×10^{-5} sec^{-1}. The effects of this decrease on the mechanical properties of the nickel, summarized in Table I, were complex although within the extremes of the data generated by samples extended at 1 mm min^{-1}. As shown in Fig. 14, the initial effect of decreasing the strain rate was to increase the average E_f and UTS values but when the rate was decreased to 5.5×10^{-5} sec^{-1} some of the E_f and UTS

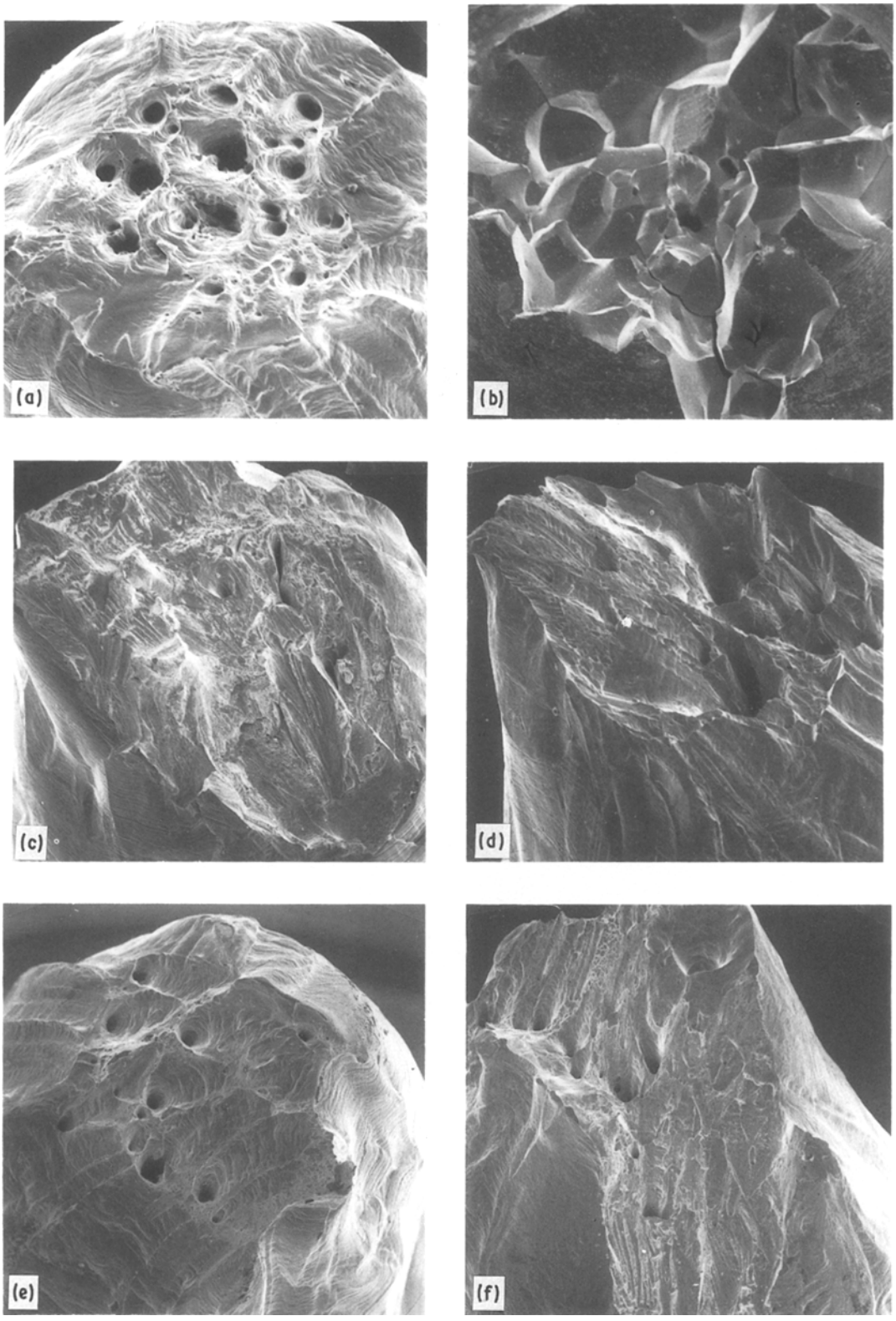

Figure 7 Fracture surfaces of samples broken in (a) argon, (b) lithium, (c) sodium, (d) potassium, (e) rubidium and (f) caesium. Lithium, ×30; sodium, ×40; others, ×50.

values fell below the scatter of those for samples strained at 1.1×10^{-3} sec^{-1}.

Decreasing the strain rate to 5.5×10^{-4} or 2.2×10^{-4} sec^{-1} caused the nickel samples to fail by mixed fracture modes. Fig. 15 shows the fracture faces of these samples to exhibit mainly transgranular cleavage but with significant areas of intergranular cleavage, and for the sample strained at 2.2×10^{-4} sec^{-1} also areas of deep dimpling. The behaviour of the samples tested using a strain rate of 5.5×10^{-5} sec^{-1} was more varied. The sample with an E_f value of 32.3% failed mainly by transgranular cleavage, but those with E_f values of 20.3% and 17.3% failed predominantly by intergranular cleavage.

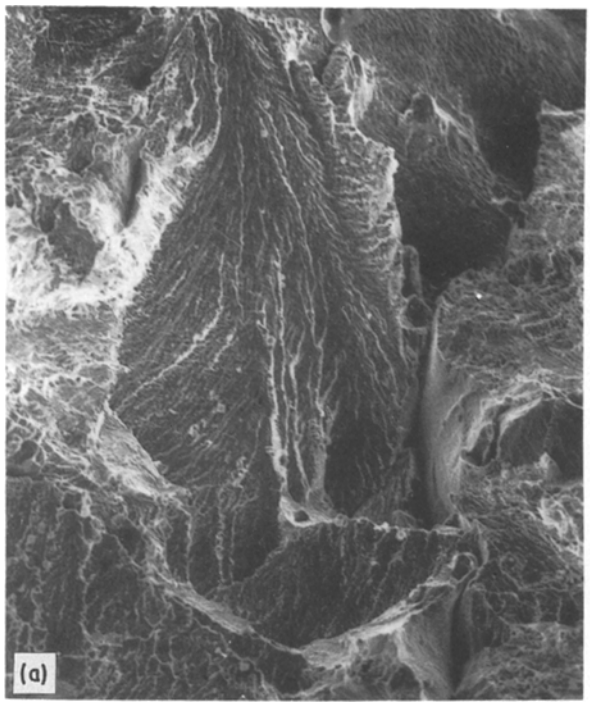

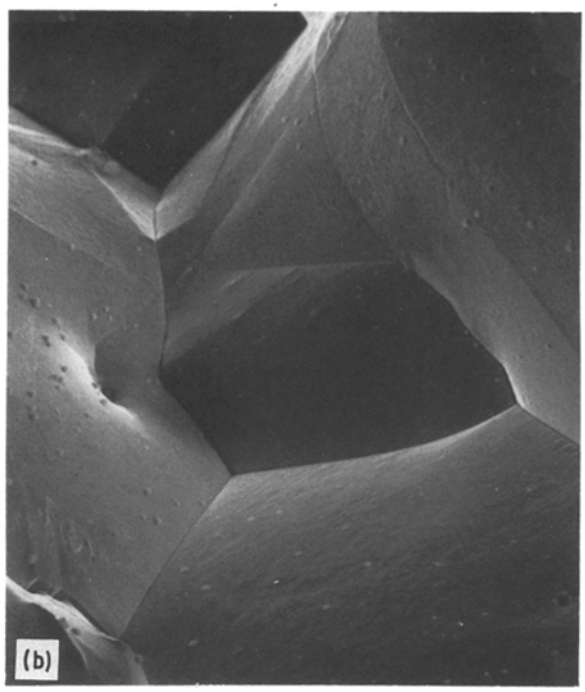

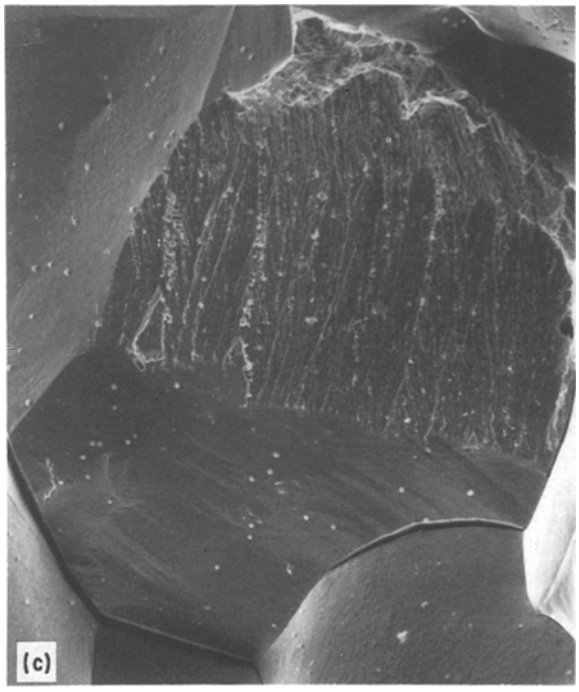

Figure 8 Fracture surfaces of nickel broken in: (a) Na, × 151. (b) Li, × 206. (c) Li, × 122.

3.4. Pre-exposure effects

The standard experimental procedure used in this work was patterned on that found necessary when working with stainless steel samples, and involved both a preheating to 450 °C to promote wetting, and a temperature stabilizing hold at 250 °C for 10 min before applying a load. To assess the importance of this pre-exposure, tensile test samples of nickel were subjected to two non-standard thermal cycles before being stressed to destruction: 120 min rather than the standard 15 min at 450 °C, and 960 min rather than 10 min at 250 °C. Non-standard exposure followed by stressing in argon had no significant effects on the mechanical properties of the samples, as summarized in Table I, while non-standard exposure and stressing in sodium–0.2% lithium caused average UTS values to decrease slightly and average E_f values to rise. However, individual UTS and E_f values all fell within the range of those observed for samples tested in sodium–0.2% lithium in the standard manner. Examination of the tensile test sample fracture surfaces revealed that failure was predominantly by intergranular cleavage but that there was also a small, less than 10%, proportion of transgranular cleavage.

4. Discussion

The prime observations of this work have been that high-purity nickel is severely embrittled by lithium, somewhat embrittled by sodium, and unembrittled by potassium, rubidium or caesium. This work therefore is in general agreement with that reported earlier for commercial quality nickel tested in lithium and sodium [9, 10] and suggests that trace impurity and segregation phenomena do not dominate the embrittling processes. However, detailed comparisons with the work of Parikh [9] and of Lynch [10] reveal minor differences in observations. The most notable of these is probably with the report by Parikh that nickel failed without yielding in lithium at 190 °C at a stress of 62 MPa, whereas we found that a stress of 107.5 MPa was required at 250 °C to produce failure after an average deformation of 6%. Parikh did not comment on the fractography of his samples, but we observed that while failure was predominantly by intergranular cleavage, there was a small amount of transgranular cleavage consistent with a modest ductility.

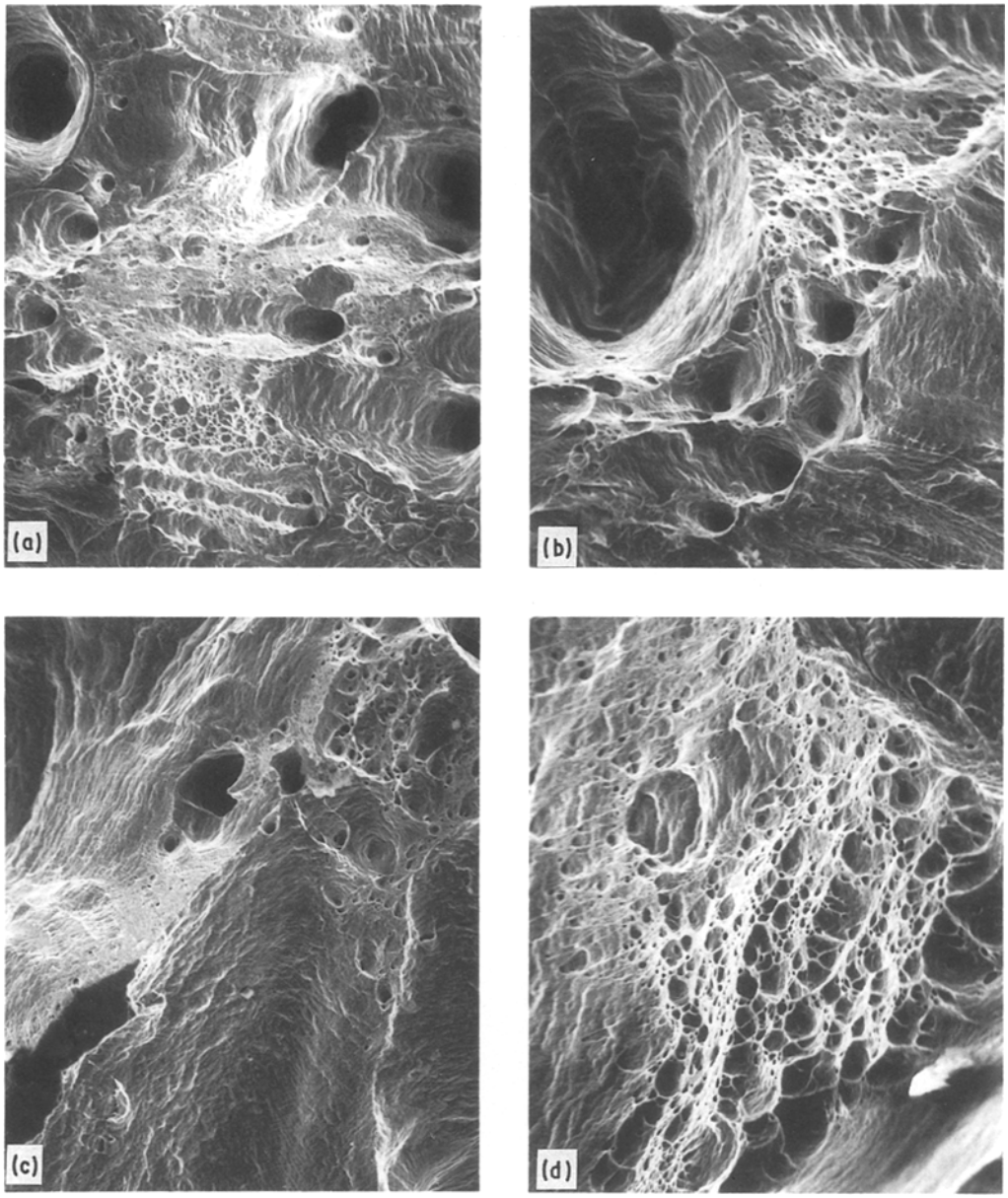

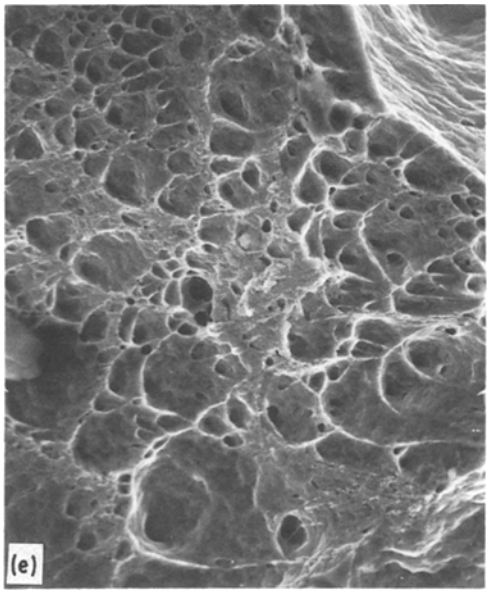

Figure 9 Fracture surfaces of nickel broken in: (a) Cs, ×152. (b) Ar, ×216. (c) Rb, ×400. (d) Ar, ×700. (e) Rb, ×1500.

Our nickel samples tested in lithium were not completely brittle, but far more so than those tested in sodium. In accord with the work of Lynch we found that intergranular and transgranular cleavage accounted for about half the fracture area of samples tested in sodium. Lynch used notched tensile test samples and concluded that sodium embrittled, but our work with smooth tensile test pieces showed that the E_f and UTS values in sodium and argon environments do not differ significantly. This comparison, therefore, suggests that crack initiation dominates the failure process in sodium. While comparative data are lacking for the other alkali metals, the measured E_f and UTS values and the fractography illustrated in Fig. 7 demonstrate the benign nature of the environments.

Empirical rules relating embrittlement to material parameters do not provide clear consistent guidance to the observed severity of lithium-induced effects. Thus Rostoker *et al.* [2] pointed out that systems displaying embrittlement seldom formed intermetallic compounds or exhibited significant mutual solubility, but while the lithium–nickel system does not form

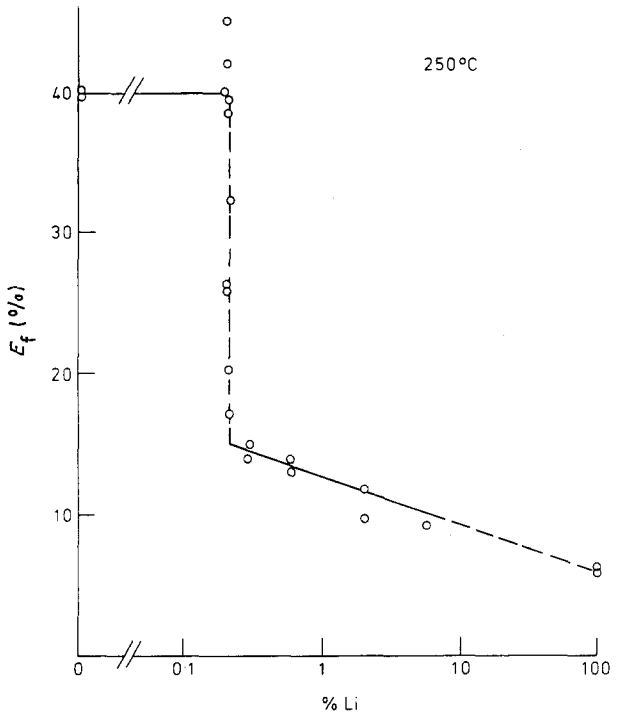

Figure 10 The ductility of nickel stressed to destruction in sodium–lithium melts.

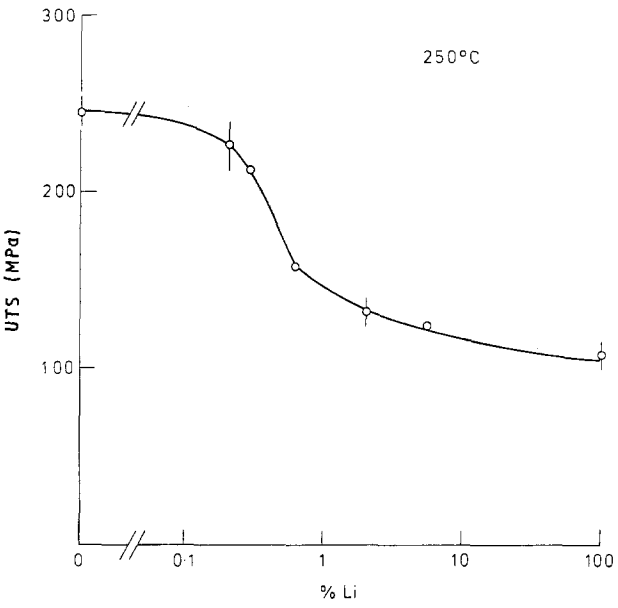

Figure 11 The strength of nickel stressed to destruction in sodium–lithium melts.

intermetallic compounds [27] the solubility of nickel is much greater in lithium than sodium [27, 29]. Again, while Westwood *et al.* [26] demonstrated for several sets of systems that similar electronegativity values could be associated with an embrittlement tendency and the electronegativity of nickel is closer to that of lithium than any other alkali metal, the difference is still so large (1.8 compared to 1.0) that embrittlement should not be expected. However, the relation of embrittlement and wetting behaviour (both of which depend on liquid–solid atom–atom interactions) does provide some consistent guidance.

Nickel is well wetted by alkali metals [30] and solid–liquid interfacial energies have been calculated for the nickel–lithium and nickel–sodium systems [31]. Using these values and the reported surface energy of nickel [32] enables estimates to be made of 2.280 J m^{-2} for nickel–argon, 0.793 J m^{-2} for nickel–sodium and 0.182 J m^{-2} for nickel–lithium for the work needed to create new surfaces as a crack propagates, while calculated heats of solution [33] suggest that the crack surface energies for nickel in potassium, rubidium and caesium will be at least as high as that in sodium. Of course this comparison ignores the very substantial contributions made by the elastic and plastic work of deformation. Nevertheless it is noteworthy that the crack surface energies rank the effects of the environments correctly and suggest that the effect of lithium may be dramatic.

Surface and interfacial energy values are also of assistance in understanding the behaviour of sodium–lithium alloys. The surface energy of molten lithium is higher than that of sodium, 0.398 as compared to 0.191 J m^{-2} at their melting temperatures [32], and hence the surface of a sodium–lithium melt should be sodium rich. Contact of nickel with a sodium-rich surface, however, will be unstable and lead to the creation of a lithium enriched lower energy interface. The initial interfacial energy will be close to the 0.793 J m^{-2} of a pure sodium melt, but whether the final value will approach the 0.182 J m^{-2} of a pure lithium melt is unknown. It can be supposed, however, that the lithium enrichment at the interface is substantial because only 0.2% lithium in sodium is sufficient to produce quite severe embrittlement of some samples, Fig. 10. Thus 0.2% lithium is a threshold at which the bulk activity is sufficient to maintain a surface concentration that decreases the interfacial energy with nickel below a critical value of about 0.7 J m^{-2}, permitting nucleation and propagation of cracks. In this context it is interesting to note that the interfacial energy for the iron–lithium system, which is ductile when carbon levels are low, is 0.733 J m^{-2} [31].

Having assigned a considerable importance to nickel–lithium atom–atom interactions, it is appropriate to consider their nature. In their calculations of interfacial energies using a Wigner–Seitz atomic cell model, Miedema and Broeder [31] found that an interactive term accounted for 11% of their value for nickel–lithium system and 82% of that for the nickel–sodium system. However, this term was not interactive in the sense that it was concerned with the formation of a new bulk phase which might initiate cracking, as does Li_2C_2 for iron [11–13]. Concern about the possible formation of this carbide and its effect on the properties of nickel prompted us to use high-purity material in this work, but even this contained 20 p.p.m. carbon. The free-energy formation of Li_2C_2 at 250 °C is $-74\,545$ J mol^{-1} [34] and hence it will be formed by contact with molten lithium if the carbon activity of the solid is 2×10^{-4} or above. The atom fraction of carbon in the nickel is 1×10^{-4} and this activity criterion could be met considering the low solubility of carbon in nickel at 250 °C [27].

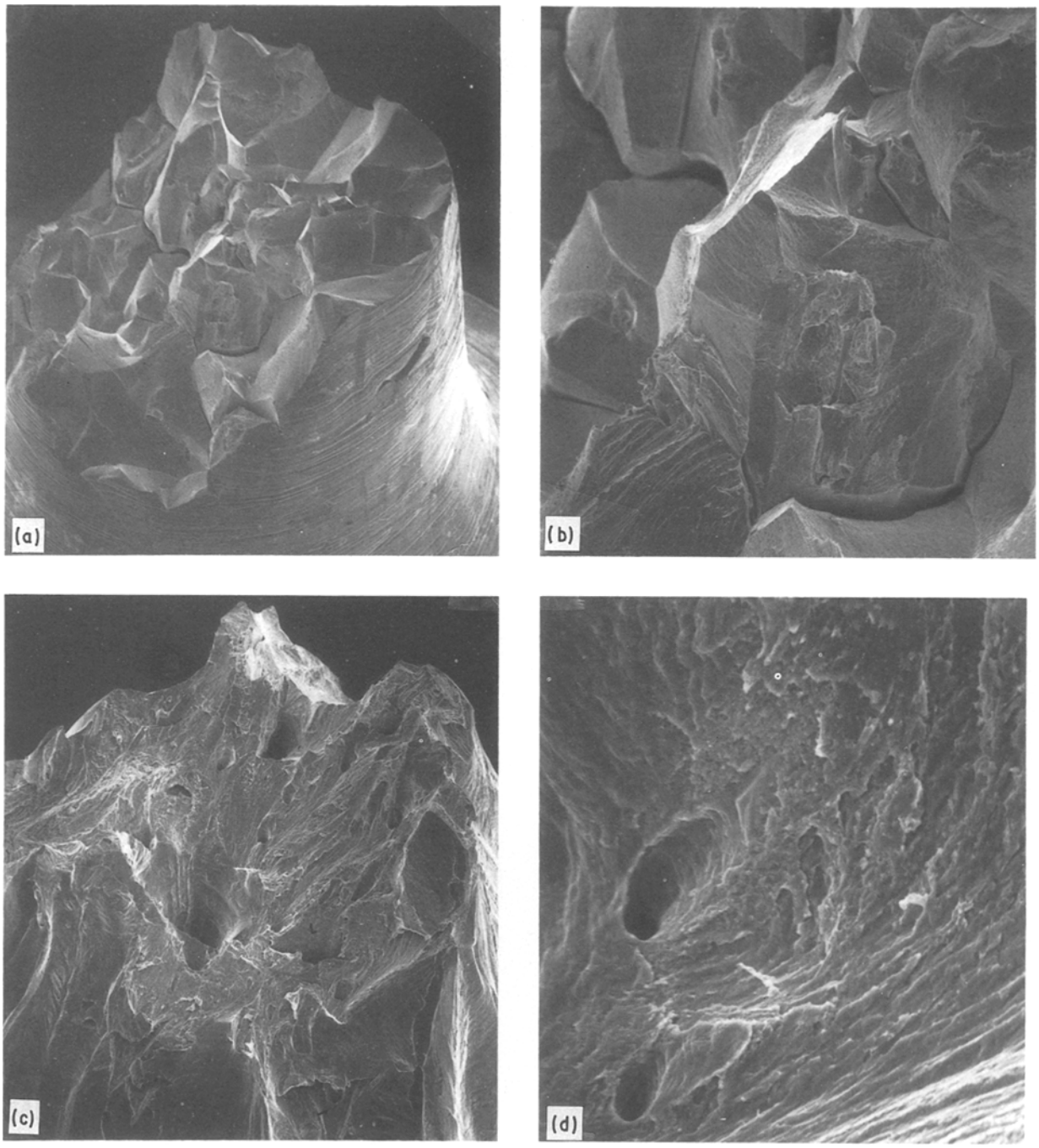

Figure 12 Fracture surfaces of nickel tests in sodium–0.2% lithium. (a) Sample 2677, E_f 25.8%, ×30. (b) Sample 2677, E_f 25.8%, ×100 (c) Sample 2676, E_f 40.0%, ×50. (d) Sample 2676, E_f 40.0%, ×1200.

The location, habit or rate of formation of Li_2C_2 could exert a major influence on the ductility of nickel, as it does for iron [11–13]. For the formation of Li_2C_2 to be significant, the reaction must give rise to needles or sheets growing along grain boundaries, but the fractographs of samples stressed to destruction in lithium provided no supporting evidence. There was some rippling of the intergranular cleavage faces but this has been observed also by Lynch [10] in more detailed studies and attributed to slip interactions and minute microvoid formation. Further, in our work, embrittlement was caused also by alloy melts containing only 0.3% lithium in sodium. Assuming an activity coefficient of unity, this concentration corresponds to a lithium activity of 5.7×10^{-3} and the formation of Li_2C_2 could then require the nickel to have a carbon activity of 3.3×10^{-2}. This activity is an enhancement of 330 over the atom fraction, a not impossible but nevertheless very high factor. The unlikelihood that a chemical reaction governed the lithium embrittlement process is also suggested by the fact that slower strain rates and prolonged prior exposure of tensile test pieces to sodium–0.2% lithium melts had no clear effect on their mechanical properties when subsequently stressed to destruction.

This work suggests that the embrittlement of nickel by lithium and lithium alloys is a physical process that does not need to be initiated by a gross chemical

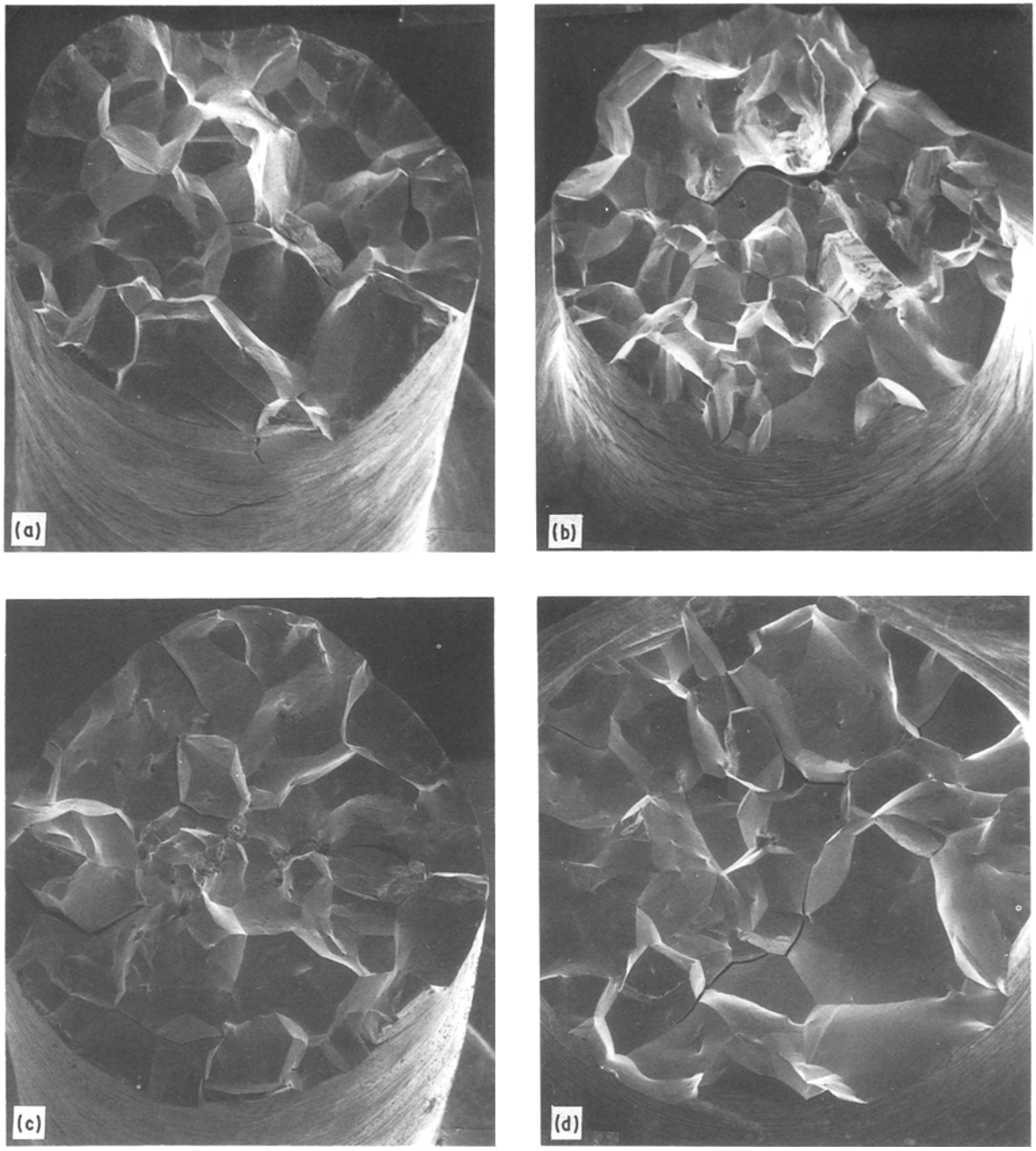

Figure 13 Fracture surfaces of nickel tested in: (a) sodium–0.3% lithium, (b) sodium–0.6% lithium, (c) sodium–2.01% lithium, (d) sodium–5.6% lithium. ×33.

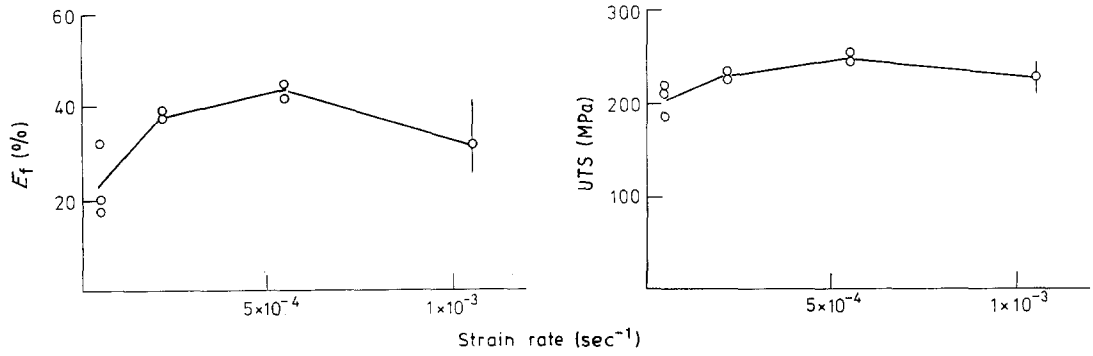

Figure 14 The influence of strain rate on the strength and ductility of nickel in sodium–0.2 lithium at 250 °C.

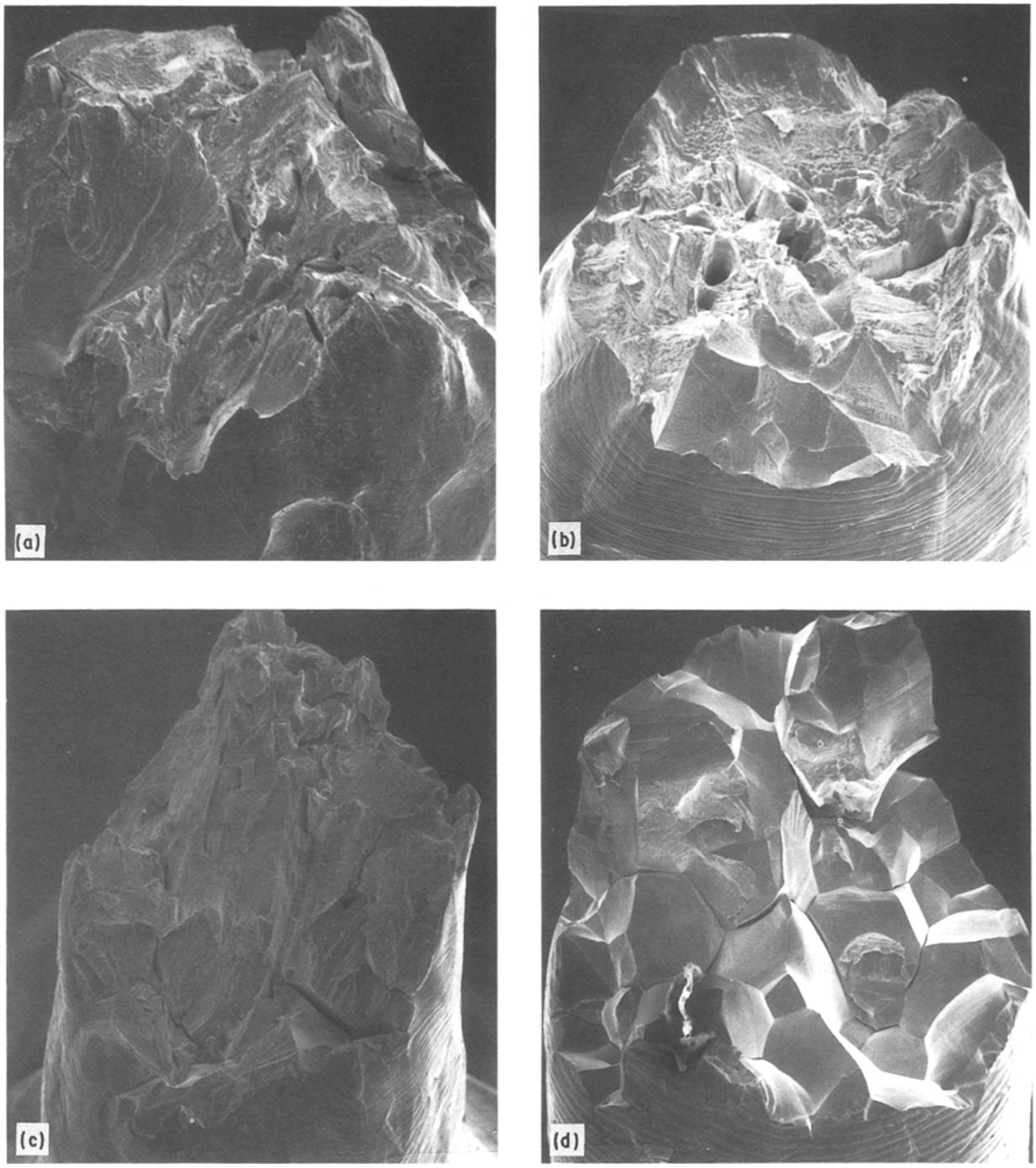

Figure 15 Fracture surfaces of nickel samples tested in sodium–0.2 lithium at: (a) 5.5×10^{-4} sec^{-1}, 45.4% E_f, ×40; (b) 2.2×10^{-4} sec^{-1}, 38.7% E_f, ×40; (c) 5.5×10^{-5} sec^{-1}, 32.3% E_f, ×30; (d) 5.5×10^{-5} sec^{-1}, 17.3% E_f, ×30.

reaction. It is therefore one of the relatively rare systems exhibiting classical LME, a form of environmentally induced brittle fracture. The outstanding characteristic of lithium–nickel among the alkali metal–transition metal systems is that it has a very low interfacial energy and this emphasizes the usefulness of regarding liquid metal embrittlement as a nucleation controlled process.

In most cases, nucleation is caused by some chemical interaction, such as the formation of Cu_4Li crystals [35] and only the subsequent propagation is classical energy-controlled liquid metal embrittlement. This work, however, shows that intergranular cleavage can be nucleated and propagate even when no apparent chemical reaction has occurred. Why a very low interfacial energy should be associated with easy nucleation is not certain, but at least two suggestions can be made. First, sharp dihedral angles will be formed by emergent grain boundaries when the interfacial energies are low compared to those of the grain boundary as illustrated in Fig. 16. For lithium–nickel the angle predicted by the Murr [32] and the Miedena and Broeder [33] data is zero and hence the resultant notch should be infinitely sharp. By comparison, the notches formed by the sodium–nickel and lithium–nickel systems should subtend angles of about 125°. However, liquid metal embrittlement can occur also with single crystals and amorphous metals [4, 7] and

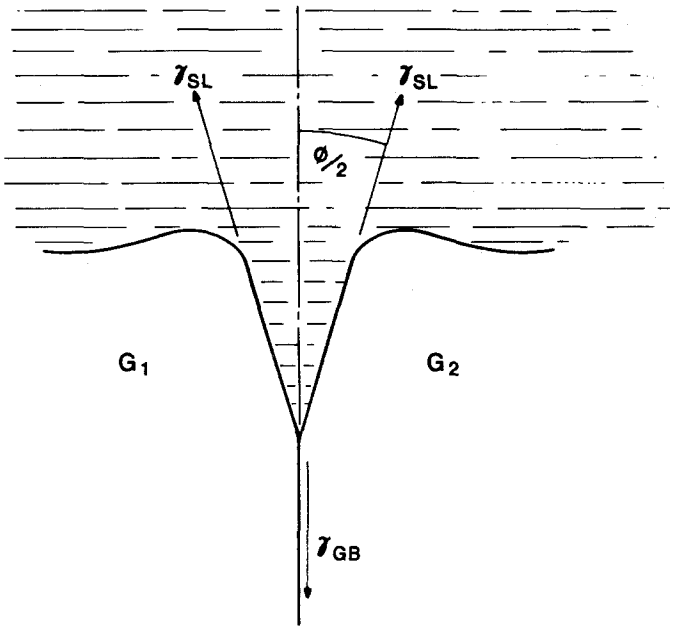

Figure 16 Equilibrium configuration of an emergent grain boundary in contact with a liquid.

hence nucleation mechanisms not dependent on grain boundaries or specific lattice features must exist. This second process could be related to temper embrittlement (which can be caused by many metals responsible for liquid metal embrittlement) and in particular to the process proposed by Briant and Messmer [36]. Wetting brings the embrittling atoms into intimate contact with the stressed solid and Briant and Messmer showed that certain foreign, temper embrittling, atoms could disrupt host lattices by perturbing the distribution of their bonding electrons.

Combined with the ease with which alkali metals can be removed from fracture faces, nickel–lithium therefore could offer attractions to future scientific investigators who wish to work with a relatively simple and characterizable system which should, for example, exhibit an upper threshold temperature dependent on grain size and strain rate at which ductility is regained. The conclusion that the embrittlement process is probably physical, however, may also have significant technological implications if this is true also for nickel alloy fusion reactor components. Freedom from chemical triggering would mean that the structure could be susceptible any time certain instantaneous criteria were satisfied and routine checking for surface damage or corrosion would be irrelevant.

Acknowledgement

Work described in this paper was undertaken as part of the Underlying Research Programme of the UKAEA.

References

1. W. H. JOHNSON, *Proc. Roy. Soc.* **23** (1874) 168.
2. W. ROSTOKER, J. M. McCAUGHEY and H. MARKUS, "Embrittlement by liquid metals" (Reinhold, New York, 1960).
3. M. H. KAMDAR, *Prog. Mater. Sci.* **15** (1973) 289.
4. N. S. STOLOFF, "Surfaces and interfaces, 2", edited by J. J. Burke (Syracuse University Press, Syracuse, 1968) p. 157.
5. M. G. NICHOLAS and C. F. OLD, *J. Mater. Sci.* **14** (1979) 1.
6. C. F. OLD, *J. Nucl. Mater.* **92** (1980) 2.
7. N. S. STOLOFF, in "Embrittlement by liquid and solid metals", edited by M. H. Kamdar (Metals Society of AIME, New York, 1984) p. 3.
8. M. G. NICHOLAS, *ibid.*, p. 27.
9. N. M. PARIKH, "Environment sensitive mechanical behaviour" (Gordon and Breach, New York, 1966) p. 563.
10. S. P. LYNCH, *J. Mater. Sci.* **21** (1986) 692.
11. J. E. CORDWELL, Proceedings of the Conference, Thomas Telford, "Liquid alkali metals" (British Nuclear Energy Society, London, 1973) p. 177.
12. V. V. POPOVICH, I. G. SHTYKALO and M. I. CHAEVSKII, *Sov. Mater. Sci.* **3** (1967) 88.
13. R. E. SPENCER, D. K. MATLOCK and D. L. OLSON, *J. Mater. Energy Systems* **4** (1983) 187.
14. C. F. OLD and P. TREVENA, *Met. Sci.* **15** (1981) 281.
15. O. CHOPRA and D. SMITH, *J. Nucl. Mater.* **123** (1984) 1213.
16. C. F. OLD and P. TREVENA, "Preliminary investigations into the possibility of liquid metal embrittlement of some ferrous alloys by sodium and lithium", AERE-R9505 (1979).
17. V. V. POPOVICH, M. S. GOIKHMAN, E. I. POLYAKOV and M. I. CHAEVSKI, *Sov. Mater. Sci.* **5** (1969) 345.
18. O. CHOPRA and D. SMITH, *J. Nucl. Mater.* **123** (1984) 1213.
19. K. NATESAN, D. L. SMITH, T. F. KASSNER and O. K. CHOPRA, "Structural materials for service at elevated temperatures in nuclear power generation", edited by A. O. Schaefer (Metals Society of AIME, New York, 1975) p. 302.
20. J. E. CORDWELL, "Tertiary creep of solution treated AISI 316 in air and sodium at 550 °C", CEGB Report RD/B/N4241 (1978).
21. J. W. MARTIN and G. C. SMITH, *Metallurgia* **54** (1956) 227.
22. M. TANAKA and H. FUKUNAGA, *J. Soc. Mater. Sci. Jpn* **18** (1969) p. 541.
23. M. G. ADAMSON, W. H. REINEKING, S. VAIDYANATHAN and T. LAURITZEN, "Embrittlement by liquid and solid metals", edited by M. H. Kamdar (Metals Society of AIME, New York, 1984) p. 523.
24. M. G. NICHOLAS, P. TREVENA and N. S. STOLOFF, Proceedings ECF6, "Fracture control of engineering structures", edited by H. C. van Elst and A. Bakker (Engineering Materials Advisory Service, Warley, West Midlands, 1986) p. 1915.
25. P. TREVENA, N. S. STOLOFF and M. G. NICHOLAS, *J. Mater. Sci.* **22** (1987) 2948.
26. A. R. C. WESTWOOD, C. M. PREECE and M. H. KAMDAR, "Fracture, 33", edited by H. Leibowitz (Academic Press, New York, 1971) p. 589.
27. T. B. MASSALSKI, "Binary alloy phase diagrams" (American Society for Metals, Metals Park, Ohio, 1986).

28. L. PAULING, "The nature of the chemical bond" (Cornell University Press, Cornell, New York, 1939).
29. T. D. CLAAR, *Reactor Technol.* **13** (1970) 124.
30. M. BARLOW and P. J. PLANTING, *Z. Metallkde* **60** (1969) 719.
31. A. R. MIEDEMA and F. J. A. BROEDER, *Z. Metallkde* **70** (1979) 14.
32. L. E. MURR, "Interfacial phenomena in metals and alloys" (Addison-Wesley, Reading, Massachusetts, 1975).
33. A. R. MIEDEMA, F. R. de BOER and R. BOOM, *Calphad* **1** (1977) 341.
34. M. W. CHASE, C. A. DAVIES, J. R. DOWNEY, D. J. FURIP, R. A. McDONALD and A. N. SYVERUD, *J. Phys. Chem. Ref. Data* **14** (1985) Supplement 1.
35. C. F. OLD and P. TREVENA, *Met. Sci.* **15** (1981) 281.
36. C. L. BRIANT and R. P. MESMER, *Studies Phys. Theor. Chem.* **48** (1987) 261.

Received 7 April
and accepted 28 September 1989